Chapter 3

Influence of lipid core material on physicochemical characteristics of ursolic acid loaded nanostructured lipid carrier: an attempt to enhance anticancer activity

Abstract: The impact of saturation and unsaturation in the fatty acyl hydrocarbon chain on the physicochemical properties of nanostructured lipid carriers (NLCs) was investigated to develop novel delivery systems loaded with an anticancer drug, ursolic acid (UA). Aqueous NLC dispersions were prepared by a high-pressure homogenization − ultrasonication technique with Tween 80 as a stabilizer. Mutual miscibility of the components at the air − water interface was assessed by surface pressure − area measurements, where attractive interactions were recorded between the lipid mixtures and UA, irrespective of the extent of saturation or unsaturation in fatty acyl chains. NLCs were characterized by combined dynamic light scattering, transmission electron microscopy (TEM), atomic force microscopy (AFM), differential scanning calorimetry, drug encapsulation efficiency, drug payload, in vitro drug release, and in vitro cytotoxicity studies. The saturated lipid-based NLCs were larger than unsaturated lipids. TEM and AFM images revealed the spherical and smooth surface morphology of NLCs. The encapsulation efficiency and drug payload were higher for unsaturated lipid blends. In vitro release studies indicate that the nature of the lipid matrix affects both the rate and release pattern. All UA-loaded formulations exhibited superior anticancer activity compared to that of free UA against human leukemic cell line K562 and melanoma cell line B16.

Langmuir 2016, 32, 9816−9825

1. Introduction

Cytotoxic anticancer drugs are more reactive, more unstable, and more diverse in terms of molecular structure and physicochemical properties than other drug classes. At the same time, their poor specificity and tendency to induce drug resistance hinder the optimal performance in the case of conventional

chemotherapy. Cancer cells exercise a variety of defense mechanisms at the cellular level to diminish the activities of chemotherapeutic agents to which they are exposed. These defense mechanisms are known as "cellular" drug resistance. The most notable is the multidrug resistance (MDR) phenotype, which involves active efflux of a broad range of cytotoxic drug molecules out of the cytoplasm by membrane-bound transporters[1-3]. In recent years; it has become more evident that the mere development of novel drugs is insufficient to guarantee progress in drug therapy.

Nanodimensional drug delivery systems possess important properties such as the increasing solubility of hydrophobic drugs and the improvement of their bioavailability[4,5]. Solid lipid nanoparticles (SLNs) combine the advantages of emulsions, liposomes, and polymeric nanoparticles; other favorable qualities of SLNs include biocompatibility[6], improved solubility, high bioavailability, controlled drug release[7,8], targeting effect on brain[9], accessibility to large scale production[10], etc. It is therefore not surprising that this relatively new class of drug carriers is quickly being adopted for the delivery of various anticancer compounds as the SLNs, comprising physiological lipids, can minimize potential toxicity and enhance efficiency[11]. However, because of the highly crystalline nature of pure solid lipids or blends of solid lipids, drugs tend to be excluded, leading to low loading capacity and drug expulsion during storage. To overcome the limitations of SLNs, nanostructured lipid carriers (NLCs) have evolved as alternatives. NLCs are usually prepared from a mixture of spatially incompatible solid and liquid lipids. Assimilation of liquid lipids increases the imperfections in the solid lipid matrix; furthermore, liquid lipids can elevate the level of drug solubilization, allowing superior accommodation for the hydrophobic drugs, which eventually enhances the drug payload and reduces the level of expulsion of the drug during storage[12-15]. A blend of solid and liquid lipids can form a stable NLC that remains in the solid state at body temperature; thus, the drug release profile can be easily modulated by varying the lipid matrix composition[16,17]. More important is the faster internalization of lipid nanoparticles into cancerous cells, leading to greater potential in cancer therapy[18-20].

NLCs comprising a mixture of saturated (solid) and unsaturated (liquid) triglycerides, phospholipids, and fatty acids may be considered as an interesting alternative to conventional combinations such as fatty acid and triglyceride, as

the blends are usually polycrystalline in nature and can enhance physical stability, encapsulation efficiency, release behavior, therapeutic efficiency, etc[17,19,21,22]. Although a number of reports about NLCs comprising saturated (solid) and unsaturated (fluid/liquid) lipids are available in the literature[12-14,23], comparative studies describing the effect of unsaturated lipids and saturated lipids on the physicochemistry of NLCs are scarce. Thus, there has been ample research in the field of NLCs, with special reference to the use of different combinations of saturated and unsaturated lipids.

Ursolic acid (UA, 3β-hydroxy-urs-12-en-28-oic acid), a natural pentacyclic triterpenoid found in different plant species[24], possesses a wide range of bioactivities, *viz*., antitumor, anti-inflammatory, antioxidant, antibacterial, antiviral, and hepatoprotective effects[25-29]. Recent studies have shown that UA has potential antitumor effects and cytotoxic activity toward various types of cancer cell lines[30-33]. In spite of such potential, the clinical application of UA is limited because of its poor aqueous solubility, resulting in its low bioavailability and poor *in vivo* pharmacokinetics. During the past decade, many approaches have been developed to improve the solubility of UA using polymeric nanoparticles[32-35], micronization[36], lipidic nanoparticles, liposomes[30,37], salt formation[38], solid dispersions[38], inclusion complexes[39,40], microemulsions and nanocrystals, etc[31]. In spite of different attempts, it has not yet been possible to develop a single optimal delivery system. Therefore, the search for novel drug delivery systems is highly warranted to improve the solubility, payload, and oral bioavailability of UA. The aim of this study was to evaluate and compare the saturated and unsaturated lipid comprising NLCs to determine if differences in composition can alter the performance of these systems. Saturated lipid [tribehenin (TB) and 2,3-di- (docosanoyloxy)propyl docosanoate], unsaturated lipid (trierucin (TE) and 2,3-bis{[(Z)-docos-13-enoyl]oxy}propyl (Z)- docos-13-enoate], saturated fatty acid [behenic acid (BA), docosanoic acid], and unsaturated fatty acid [oleic acid (OA), (9Z)-9-octadecenoic acid] were used for these studies, keeping the molar proportion of HSPC (hydrogenated soy phosphatidylcholine) constant for all the systems. Because the major drawbacks of ursolic acid are lower drug loading and poor water solubility, another objective was the development of UA encapsulated NLCs comprising different

lipid matrices to enhance drug loading, improve solubility, and increase oral bioavailability.

Surface pressure − area isotherm studies of the pure and mixed lipids as well as with ursolic acid in different combinations were conducted to determine the nature of the interactions between the lipids and the drug. Such studies can also predict the location of the drug molecules. If UA molecules prefer to stay at the interface of the NLCs, they would definitely alter the surface pressure − area isotherm of the lipid mixture. On the other hand, if the drug molecules prefer to stay in the core of the NLCs, they would hardly have any impact on the surface pressure − area isotherm of lipid mixtures. To address this issue, surface pressure − area isotherms of the lipid mixtures with varying amounts of UA were determined. The influence of different lipids on the size, polydispersity index, and ζ potential of NLCs was investigated in the absence and presence of UA. Calorimetric studies of different formulations in the absence and presence of UA were conducted with the intention of determining the impact of the composition of lipids as well as UA on the thermal behavior of NLCs. To investigate the impact of saturated and unsaturated lipids on UA entrapment efficiency (EE), loading content (LC) and release kinetics of UA-loaded formulations were also assessed. Finally, anticancer activities against human leukemic cell line K562 and melanoma cell line B16 were evaluated to determine the anticancer potential of UA-loaded NLCs. It is believed that such a comprehensive study would eventually lead to the formulation of novel drug delivery systems in the treatment of cancer and to a clearer understanding of the fundamental properties of NLCs.

2. Materials and methods

2.1. Materials

Ursolic acid (UA), tribehenin (TB), trierucin (TE), behenic acid (BA) and oleic acid (OA) were purchased from TCI Chemicals, Japan. Hydrogenated soyphosphotidylcholine (HSPC), dialysis bag (12 kDa MWCO), DMEM and RPMI 1640 medium with L-glutamine (Gibbco, USA), fetal calf serum, sodium pyruvate, HEPES, MTT [3-(4,5-dimethylthiazol-2-yl)-2,5-diphenyltetrazolium bromide] and trypsin were obtained from Sigma-Aldrich, USA. Tween 80 was purchased from Sisco Research Laboratory, India. AR grade disodium hydrogen

phosphate ($Na_2HPO_4.2H_2O$), sodium dihydrogen phosphate ($NaH_2PO_4.2H_2O$) and sodium chloride (NaCl) were the products of Merck Specialties Pvt. Ltd., India. Penicillin-Streptomycin (Biowest, Germany), Gentamycin (Nicholas, India), dimethyl sulfoxide (DMSO), sodium bicarbonate, and other chemicals/reagents were of analytical grade and purchased from local firms. All the chemicals used were stated to be ≥ 99% pure and used as received. Double distilled and HPLC grade water were used throughout the study. Human leukemic cell line K562 and mouse melanoma cell line B16 were purchased from the National Facility for Animal Tissue and Cell Culture, Pune, India. The K562 cells were maintained in RPMI 1640 and B16 cells were maintained in DMEM medium supplemented with 10 % heat inactivated FCS, 100 U/mL penicillin, 100 mg/mL streptomycin and 100 µg/mL gentamycin. Both the cultures were maintained at 37 °C in a humidified atmosphere containing 5 % CO_2. Mouse melanoma B16 cell are adherent in nature. During sub culturing of the cells this adherent property can be diminished by adding 1X trypsin solution in the cell. In all the experiments, untreated leukemic and melanoma cells were termed as control group.

2.2. Methods

Surface pressure (π) − area (A) isotherms of pure as well as mixed monolayers (solvent spread) were obtained using a Langmuir surface balance (Micro Trough X, Kibron, Helsinki, Finland). A monolayer was generated by spreading an appropriate quantity of a lipid solution dissolved in a 3:1 (v/v) chloroform/methanol mixture at the air − water interface with a Hamilton microsyringe. The solvent was allowed to evaporate for 15 min. After the generation and equilibration of the monolayer film, the barriers were compressed at a rate of 5 mm/min. NLCs were prepared by the hot homogenization − ultrasonication method as previously described[41]. Briefly, quantitative amounts of lipids (2:2:1 TB/TE: HSPC: OA/BA molar ratio) were dissolved in a 3:1 (v/v) chloroform/methanol mixture; the solvent was removed using a rotary evaporator. The thin film thus obtained was melted at 95 °C and dispersed in the preheated aqueous surfactant (Tween 80) solution. The coarse emulsion was exposed to high-speed dispersion for 1 h; the obtained pre-emulsion was sonicated for a period of 1 h with a probe sonicator (Takashi U250, Takashi

Electric) at 150 W/ kHz, maintaining the same temperature to produce nanoemulsions that were allowed to cool to room temperature to produce the NLCs, which were stored at 4 °C for further study. In the case of the drug loaded formulation, UA was premixed with the lipids while the thin film was being generated. The total lipid concentration in the dispersion was maintained at 5 mM in a 2:2:1 TB/TE: HSPC: OA/BA molar ratio, and a 10 mM aqueous nonionic (Tween 80) surfactant solution was used as a stabilizer. Different formulations drug free or loaded, were prepared. The drug concentrations were 0.125, 0.25, and 0.5 mM for all cases.

The mean particle size, population distribution, polydispersity index, and ζ potential of the NLCs were measured in a dynamic light scattering spectrometer using a Malvern Zetasizer Nano Series ZS90 instruments (Malvern Instruments, Malvern, U.K.) at 25 °C. The shape, morphology, and surface topology of the NLCs were investigated by transmission electron microscopy (TEM) (Hitachi, Tokyo, Japan) and tapping mode atomic force microscopy (AFM) (Nanoscope III, Bruker) studies[41]. Calorimetric measurements were performed using a differential scanning calorimetry (DSC) 1 STAR^e system (Mettler Toledo). The DSC studies were performed in the temperature range of − 30 to 100 °C with a scan rate of 2.5 °C/min. The phase transition temperature and other relevant thermal parameters were evaluated from the obtained DSC thermograms of respective samples using STAR^e Software version 11.00. The entrapment efficiency (EE) and drug loading (DL) were determined by the standard methods as reported previously[42]. The UA content was estimated with a UV spectrophotometer, measuring the absorbance at 214 nm. The entrapment efficiency (EE) and drug loading (DL) capacity of NLCs were calculated using the following equations:

$$EE\% = \frac{W_{TC} - W_{FC}}{W_{TC}} \times 100 \quad (1)$$

$$DL\% = \frac{W_{TC} - W_{FC}}{W_{TC} - W_{FC} + W_{TL}} \times 100 \quad (2)$$

where WTC, WFC, and WTL represent total amounts of UA, free UA, and lipid, respectively. In vitro release of UA from the NLCs was assessed using the standard dialysis bag method under sink conditions over a 96 h period.

2.3. *In - vitro* cytotoxicity study of UA-NLCs

Log phase K562 and B16 cells (1×10^5 cells, 100 µL cell suspensions) were seeded in 96-well tissue culture plates. They were treated with freshly prepared UA-loaded NLCs at different concentrations and different incubation times at 37 °C in a humidified atmosphere containing 5% CO_2. Untreated cells served as the control. The cytotoxicity studies were performed using the MTT assay, and the absorbance of the colored solution was measured at a wavelength of 492 nm for K562 and at 570 nm for B16 cells by a microplate manager (reader type, model 680 XR from Bio-Rad Laboratories Inc.). IC_{50} values were obtained at 24 and 48 h for UA-loaded NLCs.

3. Results and discussion

3.1. Interfacial behavior of the monomolecular films

Surface pressure (π) − area (A) isotherms were constructed for pure components, mixed lipids, and mixed lipids in combination with UA. In the case of the mixed lipid and UA combinations, the lipid mixture was considered component 1 while UA was considered component 2. Lift-off areas of TB, TE, HSPC, BA, OA, and UA appeared at 75.14, 164.02, 93.61, 51.22, 78.87, and 106.17 nm^2 $molecule^{-1}$, respectively. Representative isotherms are shown in Figure 1and Figure 2.

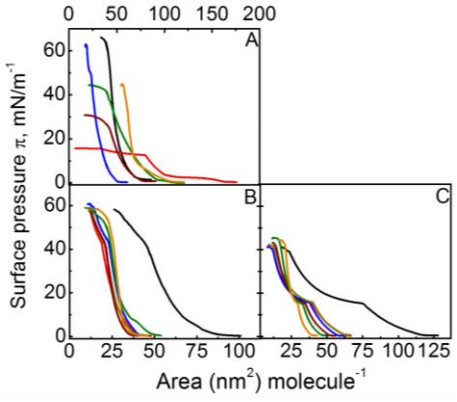

Figure 1. Surface pressure (π) – area (A) isotherm of (—), tribehenin; (—), trierucin; (—), HSPC; (—), behenic acid; (—), oleic acid and (—), ursolic acid (panel A); TB+HSPC+BA (panel B); and TE+HSPC+OA (panel C). Panel C describes the π-A isotherm of mixed monolayer in the absence and presence of ursolic acid respectively using water as subphase. Mole % of ursolic acid with respect to lipid mixture: (—), 0; (—), 2.5; (—), 5; (—), 10; (—), 30; (—), 50; and (—), 70. Temperature 25 °C.

Addition of UA resulted in a downshift in the lift-off area of the mixed monolayers; the downshift was more significant for fluid lipids (TE/HSPC/OA and TE/HSPC/BA). The condensing effect of UA, analogous to that of cholesterol[43-46], was due to the strong attractive hydrophobic and/or van der Waals interactions between the lipids and UA molecules.

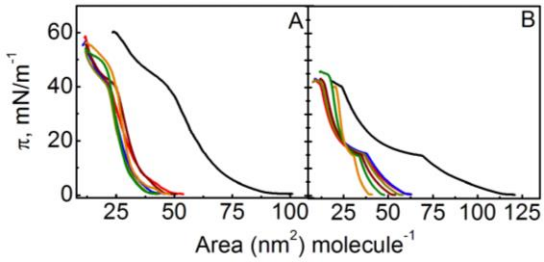

Figure 2. Surface pressure (π) – area (A) isotherm of mixed lipid and ursolic acid – lipid mixture: TB+HSPC+OA (panel A); and TE+HSPC+BA (panel B) describes the π-A isotherm of mixed monolayer in the absence and presence of ursolic acid respectively using water as subphase. Mole% of ursolic acid with respect to lipid mixture: (—), 0; (—), 2.5; (—), 5; (—), 10; (—), 30; (—), 50; and (—), 70. Temperature 25 °C.

Monolayer mechanical properties can easily be assessed by calculating the elasticity modulus (C_s^{-1}), which is the inverse of the film compressibility defined according to the following relation[47].

$$C_s^{-1} = -A\left(\frac{d\pi}{dA}\right)_T \qquad (3)$$

The profiles of the elasticity modulus versus the percent of compressed area are shown in Figure 3. For lipid mixtures in the absence of UA, maximal values were observed at 85, 79, 46, and 37 mN m^{-1} for TB/HSPC/BA, TB/ HSPC/OA, TE/HSPC/BA, and TE/HSPC/OA mixtures, respectively. C_s^{-1} values for UA/lipid mixed monolayers reveal a major reduction in the maximum, ranging from 120 to 67 mN m^{-1}, from 95 to 65 mN m^{-1}, from 75 to 30 mN m^{-1}, and from 72 to 35 mN m^{-1} for TB/HSPC/BA, TB/HSPC/OA, TE/HSPC/BA, and TE/HSPC/OA mixtures, respectively.

Such a decrease indicates a fluidizing effect of UA or the decreased elasticity of the mixed lipid monolayer; the lower the maximal value of the

elasticity modulus, the higher the fluidity of the monolayer[48]. An alteration of the molecular area of the UA molecule occupied in the monolayer, a change in the molecular packing effectiveness, and/or a change in the membrane fluidity may induce such modifications in the thermodynamic parameters.

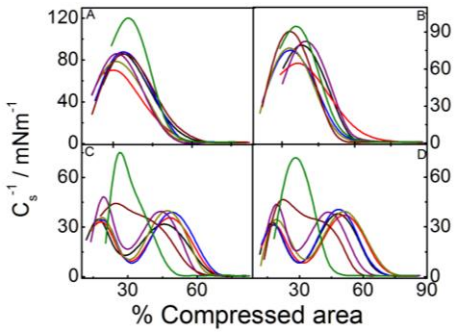

Figure 3. Variation in elasticity moduli (C_s^{-1}) with % of compressed area for mixed monolayer systems: TB+HSPC+BA (panel A); TB+HSPC+OA (panel B); TE+HSPC+BA (Panel C); and TE+HSPC+OA (panel D), lipid mixture, component 1, (2:2:1, M/M/M) and ursolic acid, component 2. Mole % of ursolic acid with respect to lipid mixture: (—) 0; (—), 2.5; (—), 5; (—), 10; (—), 30; (—), 50; and (—), 70. Temperature: 25 °C.

To gain further information about the interactions between the lipids and UA molecules, the excess area (A_{ex}), changes in the excess free energy of mixing (ΔG_{ex}), and changes in the free energy of mixing (ΔG_{mix}) of the lipid/UA monolayers were calculated from the $\pi - A$ isotherms at different surface pressures. The excess area determines if the mixing is ideal or nonideal. The ideal area of mixing is calculated using eq 4:[48]

$$A_{id} = x_1 A_1 + x_2 A_2 \qquad (4)$$

where x1 and x2 are the mole fractions and A_1 and A_2 the areas per molecule of components 1 and 2, respectively. To estimate the deviation from the ideal behavior, the excess area (A_{ex}) was calculated as[48]

$$A_{ex} = A_{12} - A_{id} \qquad (5)$$

where A_{12} represents the experimentally obtained mean molecular area. The A_{ex} value of the pseudobinary monolayer was calculated at different surface

pressures (from 5 to 30 mN m^{-1} with an interval of 5 mN m^{-1}), as shown in Figure 4.

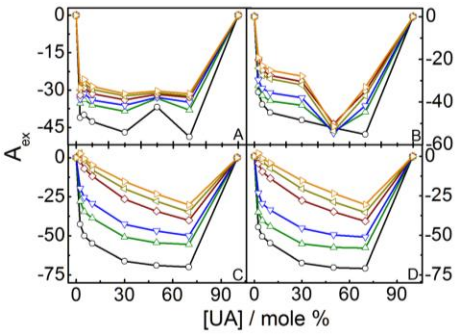

Figure 4. Dependence of excess molecular area (A_{ex}) on the relative proportion of ursolic acid in the mixed monolayer systems: TB+HSPC+BA (panel A); TB+HSPC+OA (panel B); TE+HSPC+BA (Panel C); and TE+HSPC+OA (panel D), lipid mixture, component 1, (2:2:1, M/M/M) and ursolic acid, component 2, (Mole % of ursolic acid with respect to lipid mixture): 0, 2.5, 5, 10, 30, 50, 70 and 100), at different surface pressure (mNm^{-1}): ○, 5; △, 10; ▽ 15; ◊ 20; ◁, 25 and ▷, 30. Temperature: 25 °C.

Negative deviations from the ideality for A_{ex} values were recorded for all the lipids and for all mole percents of UA in the entire studied surface pressure range, which indicate attractive interactions among the components. The magnitudes of the negative deviations were higher for the unsaturated lipid (TE) than for the saturated lipid (TB), indicating better incorporation of UA into the mixed monolayer containing unsaturated lipids.

The excess free energy that determines the degree of deviation from the ideally mixed monolayer was calculated using the following expression:[48]

$$\Delta G_{ex}^{0} = \int_{0}^{\pi} [A - (x_1 A_1 + x_2 A_2)] d\pi \qquad (6)$$

Changes in the free energy of mixing determine the thermodynamic stability of the monolayers. It can be computed from the excess free energy and the ideal free energy (ΔG_{id}) using eqs 7 and 8:[48]

$$\Delta G_{mix} = \Delta G_{ex} + \Delta G_{id} \qquad (7)$$

where the ideal free energy (ΔG_{id}) is given by

$$\Delta G_{id} = RT(x_1 lnx_1 + x_2 lnx_2) \quad (8)$$

where R is the universal gas constant and T is the absolute temperature. Negative ΔG_{ex} values, as shown in Figure 5, indicate spontaneity in the mixing processes between the components[45,48-50]. ΔG_{ex} values were more negative at higher surface pressures. The minimal ΔG_{ex} value was identified at 19, 52, 67, and 69 mol % UA for TB/HSPC/BA, TB/HSPC/OA, TE/HSPC/BA, and TE/HSPC/OA mixtures, respectively, at a π of 10 mN/m. These compositions, therefore, correspond to the most stable lipid/UA mixed films. The surface pressure increase in the loose packing density regimes, $\pi \leq 10$ mN/m (LE and LE/LC phase transitions), caused the ΔG_{ex} values of all the lipid mixtures to become more negative, because of the increase in the level of intermolecular attractive van der Waals forces.

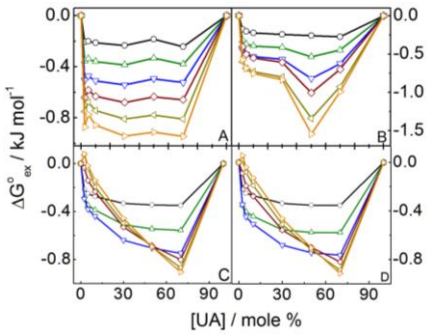

Figure 5. Dependence of change in excess free energy (ΔG^{o}_{ex}) on the relative proportion of ursolic acid in the mixed monolayer systems: TB+HSPC+BA (panel A); TB+HSPC+OA (panel B); TE+HSPC+BA (Panel C); and TE+HSPC+OA (panel D), lipid mixture: component 1, (2:2:1, M/M/M) and ursolic acid: component 2. Mole % of ursolic acid with respect to lipid mixture: 0, 2.5, 5, 10, 30, 50, 70 and 100) at different surface pressure (mNm^{-1}): ○, 5; △, 10; ▽ 15; ◊ 20; ◁, 25 and ▷, 30. Temperature: 25 °C.

The decrease in the ΔG_{ex} with an increasing mole percent of UA indicates the dependence of the packing of lipid molecules on the relative proportion of UA. A negative ΔG_{mix} value implies spontaneity in the mixing processes and strong interactions between the interfacial components, as shown in Figure 6. Negative ΔG_{mix} values were observed at all surface pressures, thus suggesting spontaneous mutual miscibility among the components. The minimal

ΔG_{mix} value was obtained at 50 mol % UA and a surface pressure of 10 mN m^{-1}, corresponding to the composition of the monolayer with the maximal thermodynamic stability.

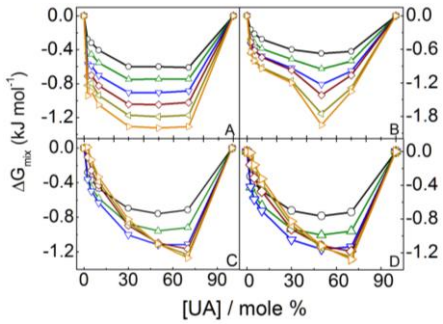

Figure 6. Changes in the free energy of mixing (ΔG^{o}_{mix}) on the relative proportion of ursolic acid in the mixed monolayer systems: TB+HSPC+BA (panel A); TB+HSPC+OA (panel B); TE+HSPC+BA (Panel C); and TE+HSPC+OA (panel D), lipid mixture, component 1, (2:2:1, M/M/M) and ursolic acid, component 2. Mole% of ursolic acid with respect to lipid mixture: 0, 2.5, 5, 10, 30, 50, 70 and 100 at different surface pressure (mNm^{-1}): ○, 5; △, 10; ▽ 15; ◊ 20; ◁, 25 and ▷, 30. Temp. 25 °C.

The dipole moment of the film-forming materials and the change in orientation of head or tail groups in the lipid monolayer as well as of the water molecules in the subphase during compression give the value of surface potential. The surface potential − area measurements have been obtained to gain information about the orientation of the film constituents. Surface potential isotherms of pure components are shown in Figure 7; the formation of mixed lipid monolayers on a subphase containing pure water with and without varying concentrations of UA is shown in Figure 8. The surface potential − area profiles were more or less similar to the surface pressure − area isotherms, further supporting the aforementioned propositions.

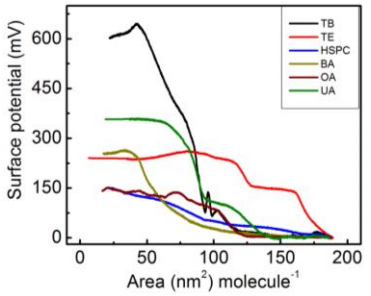

Figure 7. Surface potential of ursolic acid and pure lipid components; systems mentioned inside the figure. Pure water was used as subphase. Temp. 25 °C.

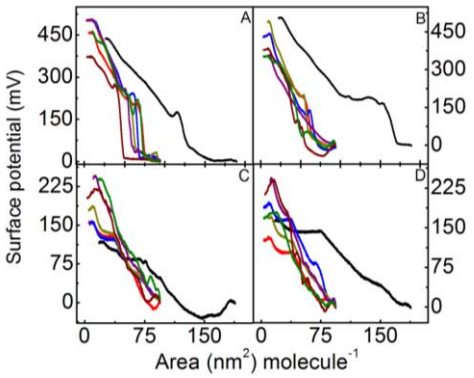

Figure 8. Variation in the surface potential of mixed lipid and ursolic acid – lipid mixture: TB+HSPC+BA (panel A); TB+HSPC+OA (panel B); TE+HSPC+BA (Panel C); and TE+HSPC+OA (panel D) describes the surface potential of mixed monolayer in the absence and presence of ursolic acid respectively using water as subphase. Mole% of ursolic acid with respect to lipid mixture: (—) 0; (—), 2.5; (—), 5; (—), 10; (—), 30; (—), 50; and (—), 70. Temp. 25 °C.

3.2. Dispersions / solution behavior of the NLCs

3.2.1. Dynamic light scattering (DLS) studies

The hydrodynamic diameter (dh), polydispersity index (PDI), and ζ potential (ZP) are some of the markers of colloidal dispersion determining its stability as well as giving insight into the in vivo performance of NLCs. NLCs comprising triglyceride, phospholipid, and fatty acids were TB/HSPC/BA, TB/HSPC/OA, TE/HSPC/BA, and TE/HSPC/OA mixtures. The TB/TE:HSPC:BA/OA molar ratio was kept fixed at 2:2:1; the overall lipid concentration was 5 mM dispersed in 10 mM aqueous Tween 80. The size of NLCs ranged from 140 to 230 nm with unimodal distributions. NLC formulations were studied up to 100 days (Figure 9). Particles were found to be fairly monodisperse, as revealed from the size distribution curves (data not shown) as well as from the PDI values (Figure 10). The sizes of TB/HSPC/BA, TB/HSPC/OA, TE/HSPC/BA, and TE/HSPC/OA NLCs were found to be 220 ± 8, 190 ± 7, 174 ± 4, and 147 ± 5 nm, respectively, with size increasing in the following order: TE/HSPC/OA < TE/HSPC/BA < TB/ HSPC/OA < TB/HSPC/BA [where the percentages of unsaturation in the fatty acyl hydrocarbon chains were 60, 40, 20, and 0, respectively (Table 1)]. Stronger association among the lipidic components in the case of unsaturated lipid and fatty acid resulted in size constriction compared to that in the saturated lipids[51,52].

Table 1. Mean size (d_h / nm), PDI, zeta potential (mV), Entrapment Efficiency (EE %) and Loading Capacity (LC %) values of empty and ursolic acid -loaded NLC.

Formulation	[UA] / mM	Size / nm	PDI	Z.P. /mV	%EE	%DL
TB+HSPC+BA	0.000	207 ±2	0.34 ±0.01	-16 ±0.4		
	0.125	208 ±1	0.34±0.009	-17 ±0.6	78.38±1.9	3.78±0.04
	0.250	210 ±3	0.35±0.001	-17 ±0.5	83.55±1.3	3.99±0.09
	0.500	235 ±5	0.37±0.003	-18 ±0.4	83.63±0.8	3.99±0.03
TB+HSPC+OA	0.000	196 ±3	0.38±0.013	-19 ±0.8		
	0.125	184±5	0.38±0.009	-15 ±0.7	80.08±0.9	3.88±0.03
	0.250	190 ±7	0.38±0.006	-17 ±0.5	85.33±1.5	4.09±0.07
	0.500	191±4	0.40±0.012	-18 ±0.1	85.56±1.7	4.09±0.04
TE+HSPC+BA	0.000	174 ±2	0.34±0.009	-19 ±0.4		
	0.125	183 ±3	0.35±0.013	-19 ±0.3	92.97±1.9	4.42±0.07
	0.250	191 ±7	0.35±0.024	-18 ±0.7	94.05±1.5	4.53±0.02
	0.500	180±2	0.35±0.005	-18 ±0.2	94.36±1.7	4.59±0.06
TE+HSPC+OA	0.000	147 ±5	0.31±0.016	-20 ±0.2		
	0.125	171 ±3	0.34±0.009	-20 ±0.4	97.14±1.8	4.67±0.09
	0.250	185±7	0.35±0.023	-20 ±0.5	99.92±1.3	4.76±0.07
	0.500	182 ±4	0.31±0.008	-19±0.3	99.38±1.5	4.76±0.02

N=3; Mean±SD,

HSPC: Hydrogenated soy phosphotidyl choline: common in all the systems.TB: Tribehenin; TE: Trierucin; BA: Behenic acid; OA: Oleic acid; PDI: Polydispersity index; EE: encapsulation efficiency; DL: drug loading; Blank NLC: NLC with no drugs; UA-NLC: NLC with drug (0.125/0.25/0.5 mM).

The DLS results thus could be correlated with the monolayer studies; the extents of negative deviation from ideality were higher among fluid lipids. An increasing amount of UA increased the size of TB/HSPC/BA and TE/HSPC/BA NLCs (Figure 9A, C). The lower multicrystallinity in the case of the lipid systems with lower degrees of unsaturation restricts the drug molecules mostly to reside on swelling of the NLC leading to an increase in d_h. On the other hand, in the case of more fluidic combinations (TB/HSPC/OA and TE/HSPC/OA), there was an initial increase in size with the addition of drug; the effect became insignificant with size variation at higher drug concentrations (Figure 9B, D).

Better incorporation and drug solubilization in the case of liquid lipids direct the drug to the core of the NLC, resulting in a significant influence of the added drug on d_h. In all cases, the size of the NLC formulations increased with time probably because of the tendency of the NLC formulations to coagulate. PDI values of <0.5 indicate homogeneity of the NLC formulation (Figure 10).

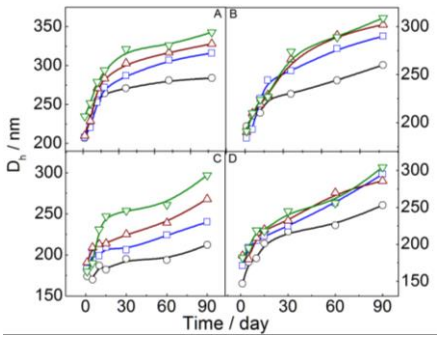

Figure 9. Variation in the hydrodynamic diameter (d_h)–time profile of NLCs Panel A: TB+HSPC+BA; panel B: TB+HSPC+OA; panel C: TE+HSPC+BA and panel D: TE+HSPC+OA. 5 mM NLC was dispersed in 10 mM Tween 80 in each case. UA concentration (mM): (○), 0; (□), 0.125; (△), 0.25 and (▽), 0.5. Temp. 25 °C.

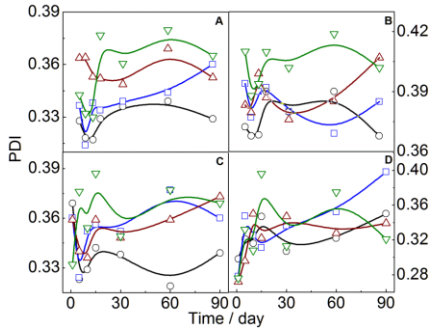

Figure 10. Variation in the polydispersity index (PDI)–time profile of NLCs Panel A: TB+HSPC+BA; panel B: TB+HSPC+OA; panel C: TE+HSPC+BA and panel D: TE+HSPC+OA. 5 mM NLC was dispersed in 10 mM Tween 80 in each case. UA concentration (mM): (○), 0; (□), 0.125; (△), 0.25 and (▽), 0.5. Temp. 25 °C.

A negative ZP was due to the dissociation of fatty acid in NLCs (Figure 11). The extent of dissociation of the incorporated fatty acid was higher for fluid lipids, for which negative values of ZP were recorded. In addition, the liquid lipid reduced d_h and consequently decreased the effective NLC surface area; thus, the ZP values for the systems having larger amounts of liquid lipids were higher. The effect of UA on the ZP of NLCs was not significant because of its nonionic nature. In all cases, the magnitude of ZP decreased with storage time (Figure 11), which was due to the structural modification of lipidic components as well as the Ostwald ripening/coagulation process, common for colloidal dispersions[53].

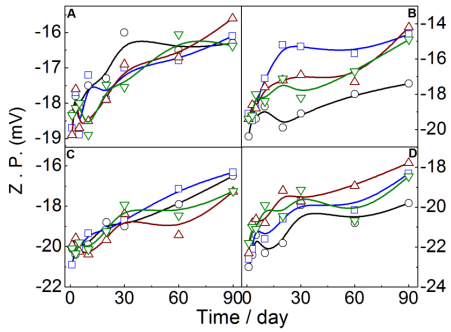

Figure 11. Variation in the zeta potential (Z.P.) – time profile of NLCs Panel A: TB+HSPC+BA; panel B: TB+HSPC+OA; panel C: TE+HSPC+BA and panel D: TE+HSPC+OA. 5 mM NLC was dispersed in 10 mM Tween 80 in each case. UA concentration (mM): (○), 0; (□), 0.125; (△), 0.25 and (▽), 0.5. Temp. 25 °C.

3. 3. Morphological studies

The size of NLCs, as evaluated from TEM studies (Figure 12), could be well correlated with particle size as determined by DLS measurements. NLCs were spherical with a smooth surface in the case of TB/HSPC/BA and TB/HSPC/OA formulations. While good contrast and distinct images were visualized in the former category, however, in the case of TE/HSPC/BA and TE/HSPC/OA formulations, contrast and distinctness were somehow reduced. It might be due the presence of a larger amount of liquid lipid in the NLC formulation. The existence of individual and distinct particles also indicates the monodisperse nature of the formulations, as was also observed by DLS[54,55].

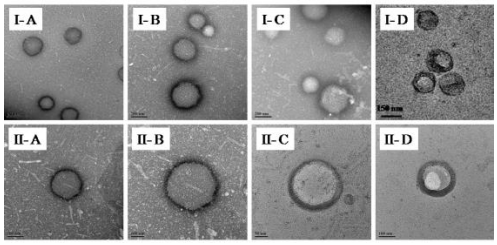

Figure 12. TEM images of NLC formulations. Composition :(A) TB+HSPC+BA; (B): TB+HSPC+OA; (C): TE+HSPC+BA and (D): TE+HSPC+OA. I and II represents the blank NLCs as well as ursolic acid loaded NLCs respectively.

Representative AFM images of TB/HSPC/BA and TE/HSPC/OA NLCs are shown in Figure 13. NLCs were found to be spherical with a smooth surface. NLCs were separated from each other, indicating the absence of aggregated

species. The observed particle sizes (200 − 230 nm) were comparable to those of the DLS and TEM studies. The particles were very distinct (Figure 13, II-A and II-B), unlike TE/HSPC/OA NLCs, whose size was found to be in the range of 160 − 200 nm, with less contrast and distinctiveness. The TB/HSPC/BA and TE/HSPC/OA NLC systems showed the observed vertical dimension to be as large as 4.1 and 2.9 nm, respectively. This could be explained by the presence of larger amounts of unsaturated lipid in the second category of NLCs than in the former.

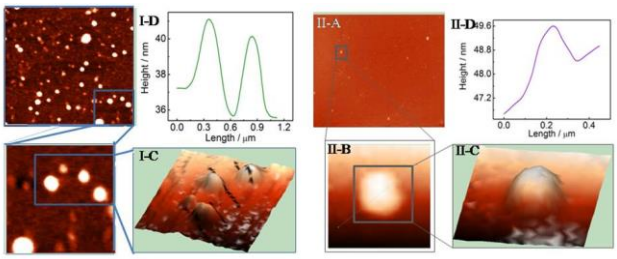

Figure 13. Representative AFM images of NLC formulation. Composition :(I) TB+HSPC+BA; and (II)TE+HSPC+OA. 2D image (A, B); 3D image (C) and section analysis (D).

3. 4. Differential scanning calorimetric (DSC) studies

Phase transition temperatures (T_m) of tribehenin, trierucin, behenic acid, oleic acid, hydrogenated soy phosphatidylcholine, and the drug ursolic acid were found to be 82.9, 30.1, 81.4, 14.3, and 283.7 °C, respectively, as shown in Figure 14. The main rationale of this study was to perceive whether the crystallinity differed in the lipid matrices due to the presence of saturation and unsaturation in their mixed states in the form of NLCs. In case of the physical mixtures (where the components were dissolved in organic solvents and subsequently dried under vacuum), the sharp peak of UA, which appeared at 283.7 °C in its pure state, disappeared (data not shown). This indicates complete solubilization of the amorphous state of ursolic acid in the lipid matrix[56]. The thermal behavior of the physical mixture of lipids and UA with lipids was also assessed (Figure 15). Tm values of the TB/HSPC/BA, TB/HSPC/OA, TB/HSPC/BA/UA, and TB/HSPC/OA/UA physical mixtures appeared at 80.1, 80.4, 77.5, and 77.8 °C, respectively (Figure 15A). Tm values of the TE/HSPC/BA, TE/HSPC/OA, TE/HSPC/BA/UA, and TE/HSPC/OA/UA physical mixtures were 27.9, 19.6,

27.8, and 20.0 °C, respectively (Figure 15B). Table 2 describes the combined thermodynamic parameters, derived from the DSC thermograms.

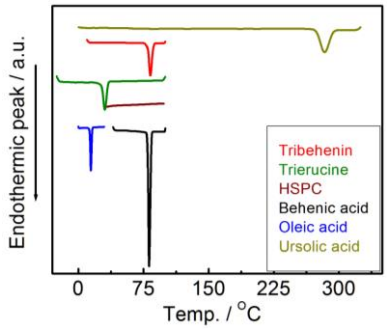

Figure 14. DSC heating thermograms of UA and the pure lipid components; systems mentioned inside the figure. Scan rate: 2.5 °C min^{-1}.

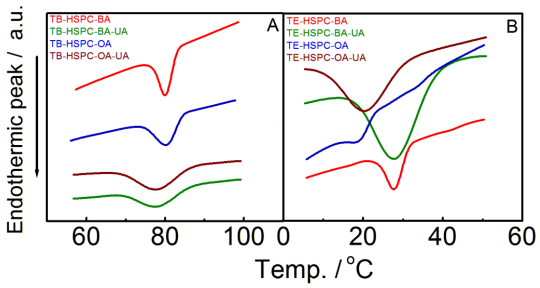

Figure 15. DSC heating thermograms of physical mixture of lipids and UA+ lipids; systems mentioned inside the figure. Scan rate: 2.5 °C min^{-1}.

The T_m value of the UA/lipid mixture, however, decreased significantly upon loading of UA into saturated lipid, which indicates a decrease in the crystallinity of the lipid matrix; this may be attributed to UA entrapment in the case of NLCs. On the other hand, the T_m values of the UA/lipid mixture did not change much with loading of UA into unsaturated lipid, although the peak was broader compared to that of the corresponding physical mixture of lipid, which may be attributed to the entrapment of UA in the NLCs. The endothermic and exothermic peaks of the physical mixtures of TB/HSPC/OA NLCs were shifted from 80 to 64 °C and from 30 to 32 °C, respectively, in the presence of UA (Figure 16). This shift was a combined effect of the inclusion of Tween 80 (on the palisade layer) as well as the drug into the core of NLCs. The endothermic peaks were taken into account to derive other associated thermal parameters, *viz*., changes in enthalpy (ΔH), heat capacity (ΔC_p), and width of the melting peak at

half-maxima ($\Delta T_{1/2}$). DSC heating curves of different lipid matrices, *viz*., TB/HSPC/ BA, TB/HSPC/OA, TE/HSPC/BA, and TE/HSPC/OA NLCs, in the presence and absence of UA are given in Figure 17.

Table 2. Temperature for maximum heat flow (T_m), the width at half peak height ($\Delta T_{1/2}$), change in enthalpy (ΔH), and heat capacity (ΔC_p) of blank as well as UA loaded NLC.

Formulation	**[UA]/mM**	**T_m/ ºC**	**$\Delta T_{1/2}$/ ºC**	**ΔH/kcal.mol^{-1}**	**ΔC_p/kcal.mol^{-1}C^{-1}**
TB+HSPC+BA	0.000	30.0	2.5	1.49	0.61
	0.125	35.4	2.5	1.81	0.71
	0.250	34.7	2.7	2.62	0.96
	0.500	34.5	2.9	3.72	1.28
TB+HSPC+OA	0.000	29.7	4.9	1.22	0.25
	0.125	30.0	6.6	4.42	0.67
	0.250	29.1	6.9	2.40	0.35
	0.500	26.6	7.5	1.61	0.22
TE+HSPC+BA	0.000	8.0	3.0	1.93	0.65
	0.125	8.6	3.2	3.39	1.06
	0.250	5.9	3.4	7.97	2.32
	0.500	4.0	4.4	9.79	2.21
TE+HSPC+OA	0.000	2.2	4.9	1.92	0.39
	0.125	4.0	5.3	2.55	0.49
	0.250	3.9	5.6	2.55	0.45
	0.500	3.7	5.8	2.52	0.43

Considering the drug free systems, significant changes in the T_m values were noted between saturated and unsaturated lipids as well as fatty acids. The T_m values were 80.1, 80.4, 27.9 and 19.6 °C for TB/HSPC/BA, TB/HSPC/OA, TE/HSPC/BA and TE/HSPC/OA physical mixture of formulations, respectively

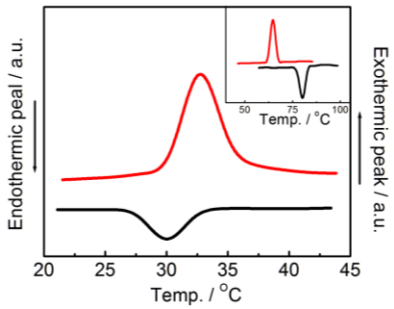

Figure 16. Representative DSC thermogram of (TB+HSPC+OA, 2:2:1 M/M/M) comprising UA-NLC and corresponded UA/lipid mixtures presented inset in the figure. Scan rate: 2.5 °C min^{-1}.

as shown in Figure 15; but were shifted to 30.0, 29.7, 8.0 and 2.2 °C for the corresponded formulated NLCs, respectively as demonstrated in Table 2. The decrease in T_m with a decrease in the size of NLCs could be explained by the Thomson proposition[41]. It has already been observed from the DLS studies that the NLCs formulated by saturated lipid and fatty acid were larger than the NLCs comprising unsaturated lipid and fatty acid. It is not unexpected that the smaller entities would have melting temperatures lower than those of the larger particles.

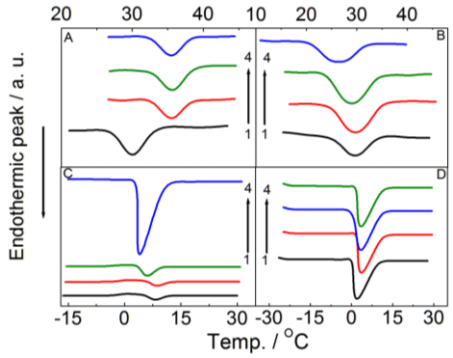

Figure 17. DSC heating curves of ursolic acid loaded NLCs. Composition of the NLCs: A: TB+ HSPC+BA; B: TB+HSPC+OA; C: TE+HSPC+BA and D: TE+HSPC+OA; [Ursolic acid]/mM: 1, 0; 2, 0.125; 3, 0.25; and 4, 0.5. Scan rate 2.5 ºC/min.

In the case of TE/HSPC/OA and TB/HSPC/BA NLCs, the phase transition temperature passed through maxima with an increasing UA concentration. These results indicate that at lower concentrations the drug molecules reside on the surface of NLCs and at higher concentrations the drug molecules are partitioned into the NLC core. In case of TE/HSPC/BA and TB/HSPC/OA NLCs, a progressive decrease in the phase transition temperature was observed with an increase in drug concentration. Increased multicrystallinity, contributed by the added drug, reduces the lowering of phase transition temperature. The liquid lipids further help the drug molecules become introduced into the core and enhance the multicrystallinity, as further supported by the increasing $\Delta T_{1/2}$ with increasing UA concentration. Incorporation of UA also increases ΔH and ΔC_p. The higher multicrystallinity led to the formation of aggregated clusters; consequently, ΔH and ΔC_p increase. In the case of TB/HSPC/OA NLCs, the extent of cluster formulation is lower because of the rigidity of NLCs. Hence, significant enhancement of the phase transition

enthalpy and heat capacity was observed at the higher drug concentration for the said NLC formulation.

3. 5. Determination of UA entrapment efficiency and drug loading capacity

Entrapment efficiency (EE) and drug loading (DL) capacity values, to estimate the quantity of UA incorporated into the NLCs, are summarized in Table 1 along with other data. The entrapment efficiency decreased in the following order: TE/HSPC/OA > TE/HSPC/BA > TB/HSPC/OA > TB/HSPC/BA (in accordance with the lipophilicity and stronger associative interaction between drugs and lipid molecules). Incorporation of the liquid fatty acid into solid lipids causes a reduction in crystallinity, consequently resulting in more imperfections in the lipid matrix and providing more space for UA molecules[16,52,57,58]. Thus, the proposition of the DSC studies was further supported by such results. The entrapment efficiency and drug loading results are well correlated with monolayer studies. With an increasing concentration of UA, a marked increase in the percentage of encapsulated drug up to 0.25 mM was recorded, beyond which it did not change appreciably.

3. 6. *In vitro* release kinetics of ursolic acid from NLC

The cumulative percentage releases of UA from NLC dispersions over 96 h are shown in Figure 18. Values for the release of UA from the TE/HSPC/OA, TE/HSPC/BA, TB/HSPC/OA, and TB/HSPC/BA formulations of 87, 78, 71, and 64%, respectively, were recorded, as presented in the inset of Figure 18. The release of UA from NLC was dependent on NLC composition[59]. A larger amount of UA was released from the unsaturated lipid blends than from the blends of saturated lipids[60]. Native UA (without any NLC, control) showed more rapid release than UA-loaded NLC, indicating sustained release of UA incorporated into NLC compared to that of native UA. Thus, the NLC dispersion could be a useful carrier with better control of UA release.

The two-step release was observed for UA loaded in all NLCs, as evidenced by the initial burst release within 3 h (39, 31, 26, and 23%) followed by a sustained release up to 96 h (87, 79, 71, and 64%). This could account for the fact that the drug encapsulation efficiency in these NLCs (i.e., matrix type or

reservoir type) and surface properties both could affect the release behavior of UA-loaded NLCs[16]. The initial burst release can be explained on the basis of the release of UA enriched in the outer shell of NLCs.

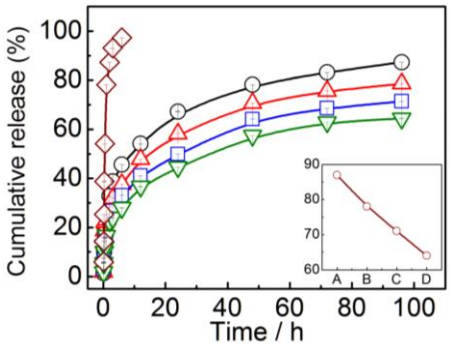

Figure 18. *In vitro* cumulative release of ursolic acid from NLCs. Composition of NLCs: TB+HSPC+BA (▽); TB+HSPC+OA (□); TE+HSPC+BA (Δ); TE+HSPC+OA (○) and free UA (◊) in PBS pH 7.4 / Tween 80 1% v/v, at 37±0.1 °C. Total release from the NLCs: (A) TE+HSPC+OA; (B) TE+HSPC+BA; (C) TB+HSPC+OA and (D) TB+HSPC+ BA. Error bars represent standard deviation (SD) of 3 different release experiments (n = 3).

3.7. *In vitro* cytotoxicity studies

In vitro cytotoxicity assays were conducted on human melanoma cell line B16 and leukemic cell line K562 by performing the MTT assay for UA upon administration in free forms or loaded in different NLCs, as shown in Figure 19. Blank NLCs did not show any significant cytotoxicity.

IC_{50} values at 24 h for free UA and UA loaded in TE/HSPC/OA and TE/HSPC/BA NLCs were 7.7, 0.041, and 0.10 μM for the B16 cell line and 224.38, 0.14, and 0.23 μM for the K562 cell line, respectively. However, the IC_{50} values of UA at 48 h when it is loaded in TB/HSPC/OA and TB/HSPC/BA NLCs were 0.062, 0.052, 0.09, and 0.19 μM for B16 and K562 cell lines, respectively. Lower IC_{50} values of UA-loaded NLCs, compared to that of free UA, suggest superior activity of the drug-loaded NLC compared to that of the free drug. Cytotoxicities of different UA-loaded NLCs comprising lipid matrices are also important attributes because UA loaded in TE/HSPC/OA and TE/HSPC/BA NLCs showed cytotoxicity higher than that in TB/HSPC/OA and TB/HSPC/BA NLCs in terms of concentration of UA and incubation time. The minimal IC_{50}

values, lower incubation times, and higher cytotoxicities for TE/HSPC/OA and TE/HSPC/BA NLCs against both the cell lines could be attributed to the fact that the higher encapsulation efficiency, faster release, and smaller size of the unsaturated lipid led to better internalization of the drug into the cell.

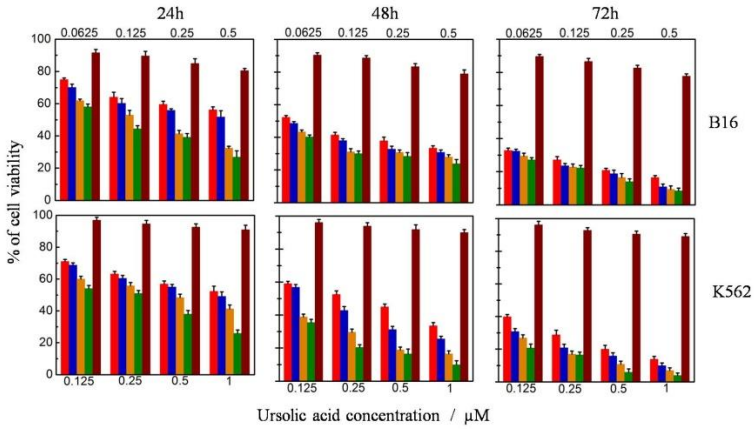

Figure 19. *In vitro* cytotoxicity activity of free ursolic acid (—) and ursolic acid loaded with different NLCs: TB+HSPC+BA (—); TB+HSPC+OA (—); TE+HSPC+BA (—) and TE+HSPC+OA (—) on the viability of B16 and K562 cell. Cell was grown and treated for 24h, 48h and 72h. Experiments were performed in triplicate, with the results showing the mean and standard deviation of the triplicate of each group. The experiments were repeated three times with similar results.

Furthermore, the capability of the formulations increased when either the concentration of UA loaded NLCs was increased or the incubation time was extended for UA-loaded NLCs. The results indicated that the anticancer activity of UA against both types of cells occurred in a concentration- and time - dependent manner. This dominance may mainly be caused by better internalization of the UA-loaded NLCs and the sustained release of UA inside the cancer cells[32]. It is worth mentioning that UA-loaded NLCs showed remarkable anticancer activities against K562 cells, which is otherwise a multidrug resistant cell line. UA-loaded NLCs thus hold the promise of overcoming multidrug resistance, and this aspect should be extensively exploited in cancer treatment.

4. Summary and conclusions

In this study, NLCs comprising saturated and unsaturated lipids and containing pentacyclic triterpenoid ursolic acid were successfully formulated. The findings

reveal the influence of saturated and unsaturated lipids and fatty acids on the particle size, polydispersity index, ζ potential, drug encapsulation efficiency, *in vitro* release behavior, and *in vitro* cytotoxicity of the formulation. The studies of surface pressure (π) − area (A) isotherms of pure components, mixed lipids, and mixed lipids with ursolic acid suggest that ursolic acid alters the interfacial organization of lipids. The spherical morphology of NLCs with a smooth surface was observed for all the formulations. Significant differences in crystal structure between NLCs comprising saturated and unsaturated lipids were noted, whereby the crystallinity of UA was lost because of its incorporation into the NLCs. Release of the drug was sustained for all the NLCs; unsaturated lipids exhibited drug release faster than that of saturated components. The most useful finding from this report is the significant difference between the cytotoxicity of free UA and UA-loaded NLCs, which demonstrates the superiority of UA-loaded NLCs over free UA in penetrating the cell membrane. UA in saturated and unsaturated lipids and fatty acid comprising NLCs showed comparable cytotoxicity in human leukemic cell line K562 and melanoma cell line B16 and enhanced anticancer activity. Conclusively, both saturated and unsaturated lipid-containing NLCs formulated in this study may be used as potential delivery systems for UA with improved anticancer activity.

References

References are given in BIBLIOGRAPHY under Chapter III (pp. 180–183).